Semiclassical Criterion for Scars in Wave Functions of Chaotic Systems

Oded Agam and Shmuel Fishman
Department of Physics, Technion, Haifa 32000, Israel
(Received 29 December 1993)

A semiclassical criterion for the existence of scars, formulated in terms of a finite number of classical periodic orbits, is shown to be useful in order to predict scarring of specific wave functions of chaotic systems, and to partly disentangle their structure. This is demonstrated by a numerical study of wave functions of a chaotic billiard that are of sufficiently high energy to be considered semiclassical.

PACS numbers: 05.45.+b, 03.65.Sq

One of the most striking ways in which the underlying classical dynamics of a chaotic system presents itself in the corresponding quantum behavior is the "scar" phenomenon. One could expect that highly excited states of chaotic systems correspond to Wigner functions which are homogeneous over the energy shell [1]. This picture is also supported by theorems of Shnirelman [2] and Colin de Verdière [3] which state that in the semiclassical limit the expectation value of an operator is almost always the microcanonical average of the classical function corresponding to the operator. However, Heller [4] found that wave functions of the stadium billiard were often strongly peaked near unstable periodic orbits. This was confirmed later on and extended to other systems such as presented in [5,6] and the references therein. Moreover, scars were directly detected in experiments on microwave cavities [7], and indirectly for hydrogen atoms in microwave fields [8]. Recently, it was argued that fluctuations in the magnetic response of mesoscopic systems may also be associated with scars [9]. In this Letter the "scar" phenomenon is quantified. For this purpose the scar weight is introduced and expressed in terms of classical periodic orbits. By calculating the scar weights one is able to predict which wave functions are scarred on the basis of purely classical information.

The natural framework for the investigation of scars is clearly the semiclassical theory. Of central importance in this theory is Gutzwiller's trace formula which expresses the density of states of a chaotic system in terms of a sum over its classical periodic orbits [10]. The problem is that this sum is not absolutely convergent for any real energy. Considerable progress towards the resolution of this difficulty has been made by introducing the spectral determinant, $\Delta(E)$, whose zeros coincide with the energy spectrum. In the semiclassical approximation it is expressed as a sum over pseudo-orbits which are linear combinations of the periodic orbits. This sum suffers from the same divergence problems as the sum for the density of states. However, several resummation methods show that it is effectively truncated after a finite number of pseudo-orbits [11,12]. The leading term of the formula obtained by Berry and Keating [12] is

$$\Delta(E) \simeq \mathrm{Re}\sum_{\mu} c_\mu e^{-i\pi\bar{N}(E)+\frac{i}{\hbar}\mathcal{S}_\mu}\mathrm{Erfc}\left\{\frac{\mathcal{S}_\mu - \pi\frac{\partial}{\partial\frac{1}{\hbar}}\bar{N}(E)}{B(K,\hbar,E)\sqrt{2\hbar}}\right\}. \tag{1}$$

where μ, which stands for a set of repetition numbers $\{r_p\}$, labels the pseudo-orbits; $\mathcal{S}_\mu$ is the pseudo-orbit action, $\mathcal{S}_\mu = \sum_p r_p S_p$, where S_p is the pth primitive orbit action, while c_μ are the pseudo-orbits amplitudes, and $\bar{N}(E)$ is the mean level staircase. The complementary error function term in this formula effectively truncates the sum to orbits with period smaller than half of the Heisenberg time. The width of the truncation region is determined by $B(K,\hbar,E) = K^2 + i\frac{\pi}{\hbar}\frac{\partial^2}{\partial(\frac{1}{\hbar})^2}\bar{N}(E)$, where K is a free fine tuning parameter.

Developing a semiclassical theory for wave functions of chaotic systems is a somewhat more delicate problem. It was first analyzed in the framework of periodic orbit theory by Bogomolny in configuration space [13], and later on by Berry in phase space [14]. However, in order to obtain convergent sums they had to introduce smearing over some energy interval. Recently, a semiclassical resummed formula for the Wigner functions of chaotic systems was derived [15] with the help of the method of [12].

For systems with 2 degrees of freedom, the semiclassical expression for the Wigner function corresponding to the eigenstate ψ_α is [15]

$$W_\alpha(\mathbf{x}) \simeq \frac{4\pi A(\mathbf{x},E_\alpha)}{h^2\Delta'(E_\alpha)}\left\{\frac{1}{4}\Delta_i(E_\alpha) + \mathrm{Re}\sum_{p,n}\Delta^{(p,n)}(E_\alpha)g_p^{(n)}e^{\frac{i}{\hbar}\tilde{\mathbf{X}}\mathbf{R}_\mathbf{p}\mathbf{X}}\right\}. \tag{2}$$

Here E_α is the corresponding eigenenergy and $\Delta'(E) = \frac{d\Delta(E)}{dE}$. The function $A(\mathbf{x},E)$ [Eq. (3.8) in [15]] accounts for an Airy fringes pattern that is encountered upon moving the phase space point $\mathbf{x} = (\mathbf{q},\mathbf{p})$ perpendicular to the energy surface $E = \mathcal{H}(\mathbf{x})$, where $\mathcal{H}$ is the Hamiltonian. The term in the curly brackets consists of a constant term which is proportional to the function $\Delta_i(E)$ that is equal to the imaginary part of the sum on the right-hand side (RHS)

0031-9007/94/73(6)/806(4)$06.00

of (1), and contributions from periodic orbits. The function $\Delta^{(p,n)}(E)$ is associated with the primitive orbit p. It is expressed as a sum over pseudo-orbits,

$$\Delta^{(p,n)}(E) = -i\sum_{\mu} c_{\mu}^{(p,n)} e^{-i\pi\bar{N}(E)+\frac{i}{\hbar}\mathcal{S}_{\mu,p}} \mathrm{Erfc}\left\{\frac{\mathcal{S}_{\mu,p} - \pi\frac{\partial}{\partial\frac{1}{\hbar}}\bar{N}(E)}{B(K,\hbar,E)\sqrt{2\hbar}}\right\}, \tag{3}$$

where $\mathcal{S}_{\mu,p} = \mathcal{S}_{\mu} + S_p$ are the pseudo-orbit actions, and $c_{\mu}^{(p,n)}$ are the amplitudes which were calculated in [15]. The spatial structure near the pth primitive orbit is mainly determined by the $n=0$ term, while the higher values of n correspond to higher powers of e^{-u_p} where u_p is the stability exponent. It is proportional to $\Delta^{(p,0)}(E)$ and it has a form of quadratic fringes $e^{\frac{i}{\hbar}\tilde{\mathbf{X}}\mathbf{R}_\mathbf{p}\mathbf{X}}$ where $\mathbf{X} = (Q,P)$ is the coordinate on the Poincaré surface of section along the orbit, and $\mathbf{R_p}$ is a two by two matrix [Eq. (3.14) of [15]] which depends only on the eigenvectors of the linearized motion on the surface of section. The higher corrections with $n>0$ are, in addition, multiplied by a polynomial function $g_p^{(n)}$ of order n of the argument $\frac{i}{\hbar}\tilde{\mathbf{X}}\mathbf{R_p}\mathbf{X}$.

The term "scar" will now be quantified. For this purpose it is useful to define the weight of a scar as the integral of the Wigner function $W_\alpha(\mathbf{x})$ over a narrow tube which surrounds the periodic orbit in phase space, and to subtract the contribution of the background. One sees from (2) that the contribution associated with a given periodic orbit is concentrated in a small region surrounding the orbit, since the contribution from more distant parts averages out to zero. The size of this region on the Poincaré surface is of order h. Therefore, if the tube is wide enough, the integral over the contribution to $W_\alpha(\mathbf{x})$ associated with the pth orbit can be calculated semiclassically. Denoting this contribution by $Y_p(E_\alpha)$ one obtains

$$Y_p(E_\alpha) \simeq \frac{T_p}{\hbar\Delta'(E_\alpha)}\Lambda_p(E_\alpha) \tag{4}$$

with

$$\Lambda_p(E) = \mathrm{Re}\sum_{n=0}^{\infty}\Delta^{(p,n)}(E),$$

where T_p is the period of the primitive orbit p. This expression does not measure the actual weight of the scar, since in the same tube there may be contributions from other orbits which are not taken into account. However, due to the normalization of the Wigner function, if $Y_p(E_\alpha)$ is of order unity, ψ_α is expected to be scarred along the pth orbit. In this case the scar weight may be approximated by $Y_p(E_\alpha)$. In the more general case, ψ_α is predicted to be scarred if a considerable part of the weight is concentrated on few $Y_p(E_\alpha)$ that are much higher than the rest. Then the scarring pattern is expected to be more complicated.

The contributions from the periodic orbits as well as those associated with the background are interrelated. This is a consequence of the normalization of the Wigner function which leads to the sum rule,

$$\Delta'(E_\alpha) = \sum_p \frac{T_p}{\hbar}\Lambda_p(E_\alpha) + \pi\bar{d}(E_\alpha)\Delta_i(E_\alpha), \tag{5}$$

where $\bar{d}(E)$ is the mean density of states. Notice that the scar weight is measured relative to the background [that is, proportional to $\Delta_i(E_\alpha)$]. A large negative value of $Y_p(E_\alpha)$, therefore, corresponds to a situation in which the probability density in the vicinity of the periodic orbit is small, i.e., to an antiscar.

For billiards, (2) is inapplicable for the calculation of Wigner functions [6]. Nevertheless, the expression for the scar weight (4) holds in this case as well. It may be derived from an extension of [14] to billiards [16].

The model which will be explored numerically in what follows is a variant of the hyperbola billiard studied extensively by Sieber and Steiner [17]. It consists of a particle of mass m moving in a two dimensional billiard illustrated in Fig. 1. The classical motion of this system is known to be completely chaotic. The eigenstates of the system may be classified according to the C_{4v} symmetry group. The results that will be presented correspond to the class of the wave functions which vanish on the boundary of the fundamental domain shadowed in the figure. The units $2m=\hbar=1$ are used.

The semiclassical spectral determinant of this system, calculated using (1), is depicted in Fig. 2. The calculation involves 17 347 primitive orbits which are the shortest among those that bounce the boundary up to 13 times.

The weights $Y_p(E_\alpha)$, calculated for the orbits $(-)$ and

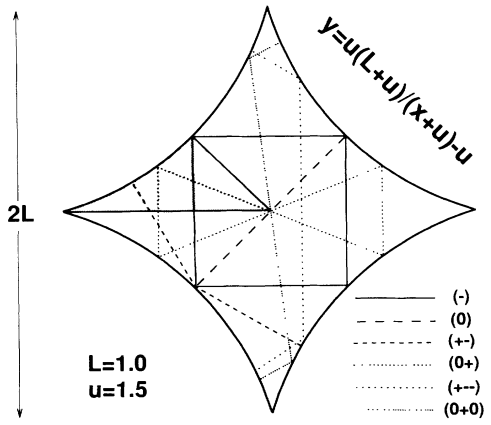

FIG. 1. The billiard model used for numerical calculations together with 6 of its periodic orbits. The shadowed area marks the fundamental domain.

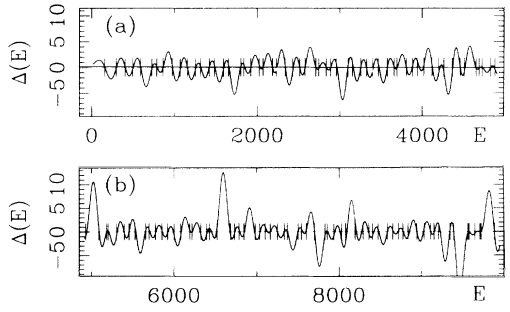

FIG. 2. The semiclassical spectral determinant (1) of the billiard shown in Fig. 1. The vertical bars along the energy axis indicate the position of the exact eigenvalues (122 of them).

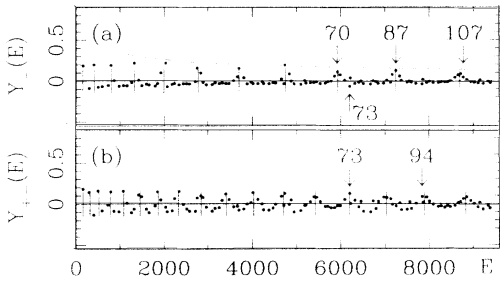

FIG. 3. The scar weights of the orbits (−) and (+−) calculated from (4). The vertical bars are located at the energies $\bar{E}_n$ which allow standing waves along the orbits. The dashed line is the approximation (6) for the peak amplitude.

(+−), are plotted in Fig 3. These are evaluated on the semiclassical approximation for the energy spectrum (Fig. 2). A clear feature of this figure is the periodicity structure of the peaks along the energy axis. These peaks may be intuitively associated with the set of energies $\{\bar{E}_n\}$ which allow "standing waves" along the periodic orbit, i.e., those which satisfy the quantization condition $S_p(\bar{E}_n)=2\pi\hbar n+\gamma_p\hbar$, where n is an integer and γ_p is the Maslov phase.

The amplitudes of the peaks of the least unstable orbit may be estimated assuming its contribution to the Wigner functions to be the dominant one. Substituting the sum rule (5) into (4), and using the diagonal approximation and the Hannay and Ozorio de Almeida sum rule [18] in order to estimate the contribution from all the other orbits, one obtains

$$Y_p(E)=\frac{1}{1+C}, \tag{6}$$

with

$$C\approx\pi\hbar u_p\bar{d}(E)/T_p,$$

where u_p is the instability exponent of the pth orbit. It is represented by the dashed line in Fig. 3(a). For two dimensional billiards $\bar{d}(E)$ is approximately constant while T_p is inversely proportional to $\sqrt{E}$. Thus the scar weights decrease as $1/\sqrt{E}$ in the limit $E\to\infty$. Nevertheless, large weights may also be found at relatively high energies since there $Y_p(E)$ is inversely proportional to u_p. Thus, as the instability of the orbit decreases its scar weights increase and the energy interval at which they appear becomes wider.

The densities corresponding to several wave functions numbered and indicated by arrows in Fig. 3(a) are shown in Fig. 4. These are scarred by the orbit (−) drawn by a thick line. The thin lines on both sides of the periodic orbits mark a strip of width that is twice the wavelength λ where the contribution from the periodic orbit is expected to be large. Although all these functions are scarred along the same periodic orbit, their precise shape within the tube is very different.

Most of the fine details of the scarring pattern probably cannot be explained in the framework of semiclassical theory. However, some of them result from interference with other scars. For instance, the wave function No. 94 shown in Fig. 5(a) is scarred by mainly two orbits, (+−) and (+ − −), drawn by the solid and the dashed lines, respectively. At regions where the separation between the two orbits is less than a few wavelengths, a strong enhancement of the density is observed, and the scarring pattern is washed out. It is easily recognized where the two orbits are sufficiently separated. A different interference pattern appears when it involves a scar and an antiscar, as shown in Fig. 5(b), where the density corresponding to the wave function No. 73 is plotted. The antiscar along the orbit (−) [see Fig. 3(a)] is designated

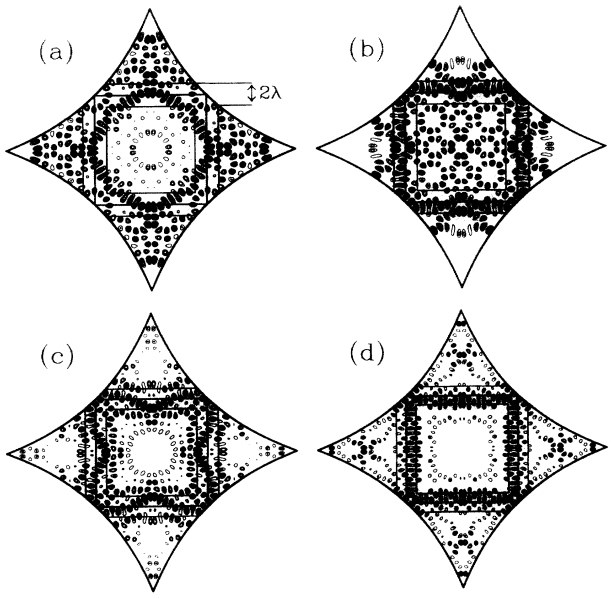

FIG. 4. The densities of the wave functions Nos. (a) 70, (b) 71, (c) 87, and (d) 107 scarred by the orbit (−). The corresponding weights are indicated by arrows in Fig. 3(a).

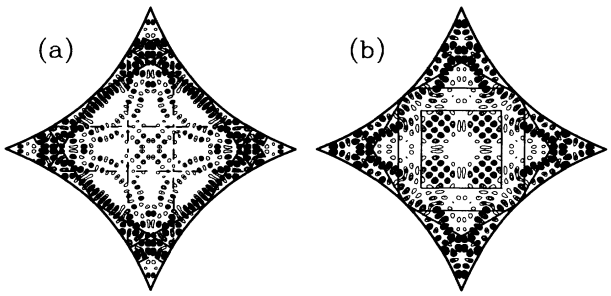

FIG. 5. The densities of the wave functions: (a) No. 94 scarred by the orbits (+−) and (+ − −); (b) No. 73 scarred by (+−) and antiscarred by (−).

by the tube which surrounds this orbit, while the orbit (+−) that scars the wave function [see Fig. 3(b)] is drawn by a thick line. The structure of the wave functions is expected to become more obscure as the number of scars and antiscars with large weights increases. In such cases these terms may become meaningless.

The above procedure was repeated for many wave functions. Plots of the type presented in Fig. 3 were used to predict and identify which wave functions are scarred by specific orbits. Then the densities were plotted (as in Figs. 4 and 5) and examined visually. All the wave functions that were predicted to be scarred by *specific* orbits were indeed found to be scarred by these orbits. In the present work, 18 wave functions scarred according to these predictions were obtained with *no* counterexample. Therefore the likelihood ratio for the validity of this criterion relative to its complete irrelevance, namely, to a situation in which the regions where the densities are large are totally unrelated to the specific classical periodic orbits, as predicted in this work, is $\mathcal{L} = 2^{18}$. It was obtained assuming that if the scarring criterion is wrong, the probability to find by pure chance that a *specific* wave function is scarred by the periodic orbit that is predicted is 1/2. The likelihood ratio $\mathcal{L}$ is the measure of statistical significance of the verification of the scar criterion [19].

In this work the term "scar" has been quantified by introducing the scar weight which measures for an eigenstate the excess probability of the system to be in a small tube surrounding a given classical periodic orbit in phase space. In the semiclassical limit this weight is expressed in terms of a finite number of classical periodic orbits. It therefore provides a way for predicting which of the wave functions is scarred or antiscarred on the basis of purely classical information. This was verified numerically for a chaotic billiard. Moreover, it was demonstrated that the gross features of the scarring pattern may be characterized by the *set* of scar weights $\{Y_p(E_\alpha)\}$.

We are grateful to N. Brenner, E. J. Heller, and S. Tomsovic for very informative discussions. This work was supported in part by the U.S.-Israel Binational Science Foundation (BSF), and by the Fund for Promotion of Research at the Technion.

[1] M. V. Berry, J. Phys. A **10**, 2083 (1977); A. Voros, in *Stochastic Behavior in Classical and Quantum Hamiltonian Systems*, edited by G. Casati and J. Ford, Lecture Notes in Physics Vol. 93 (Springer, Berlin, 1979), pp. 326–333.
[2] A.I. Shnirelman, Usp. Mat. Nauk. **29**, No. 6, 181 (1974).
[3] Y. Colin de Verdière, Commun. Math. Phys. **102**, 497 (1985).
[4] E. J. Heller, Phys. Rev. Lett. **53**, 1515 (1984); in *Quantum Chaos and Statistical Nuclear Physics*, edited by T. H. Seligmann and H. Nishioka, Lecture Notes in Physics Vol. 263 (Springer, Berlin, 1986), p. 162.
[5] D. Wintgen and A. Hönig, Phys. Rev. Lett. **63**, 1467 (1989); B. Eckhardt, G. Hose, and E. Polak, Phys. Rev. A **39**, 3776 (1989).
[6] M. Feingold, R. G. Littlejohn, S. B. Solina, and J. S. Pehing, Phys. Lett. A **146**, 199 (1990).
[7] J. Stein and H.-J. Stöckman, Phys. Rev. Lett. **68**, 2867 (1992); S. Sridhar and E. J. Heller, Phys. Rev. A **46**, 1728 (1992).
[8] R. V. Jensen, M. M. Sanders, M. Saraceno, and B. Sundaram, Phys. Rev. Lett. **63**, 2771 (1989).
[9] O. Agam, J. Phys. I (France) **4**, 697 (1994).
[10] M. C. Gutzwiller, J. Math. Phys. **8**, 1979 (1967); **10**, 1004 (1969); **11**, 1791 (1970); **12**, 343 (1971).
[11] P. Cvitanovič and B. Eckhardt, Phys. Rev. Lett. **63**, 823 (1989); E. B. Bogomolny, Nonlinearity **5**, 805 (1992); E. Doron and U. Smilansky, Nonlinearity **5**, 1055 (1992).
[12] M. V. Berry and J. P. Keating, Proc. R. Soc. London A **437**, 151 (1992).
[13] E. B. Bogomolny, Physica (Amsterdam) **31D**, 169 (1988).
[14] M. V. Berry, Proc R. Soc. London A **423**, 219 (1989).
[15] O. Agam and S. Fishman, J. Phys. A **26**, 2113 (1993); corrigendum in J. Phys. A **26**, 6595 (1993).
[16] O. Agam (to be published).
[17] M. Sieber and F. Steiner, Physica (Amsterdam) **44D**, 248 (1990).
[18] J. H. Hannay and A. M. Ozorio de Almeida, J. Phys. A **17**, 3429 (1984).
[19] We thank P. Cvitanovič for insisting on a statement of the statistical significance of the test presented in this work.

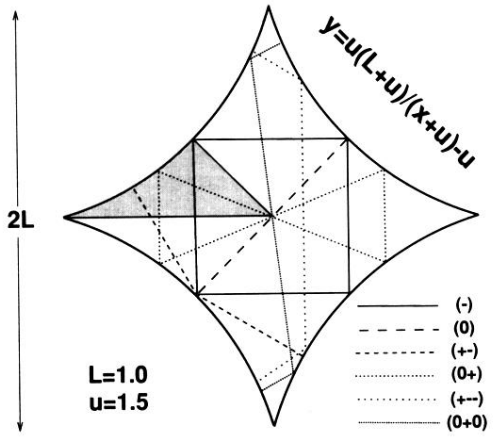

FIG. 1. The billiard model used for numerical calculations together with 6 of its periodic orbits. The shadowed area marks the fundamental domain.

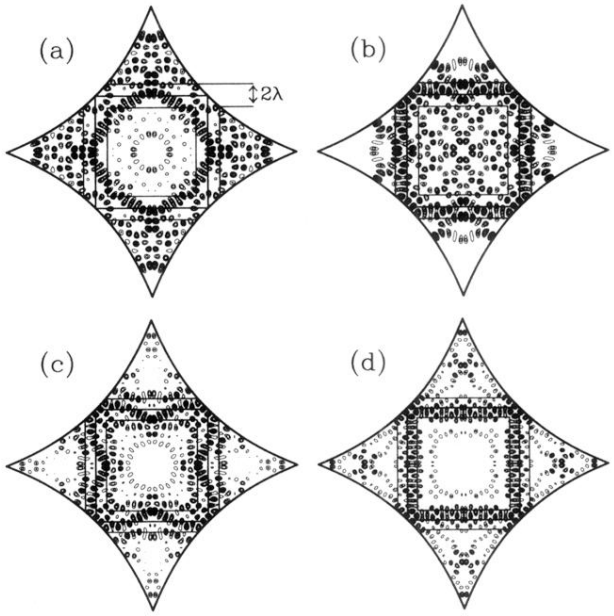

FIG. 4. The densities of the wave functions Nos. (a) 70, (b) 71, (c) 87, and (d) 107 scarred by the orbit (−). The corresponding weights are indicated by arrows in Fig. 3(a).

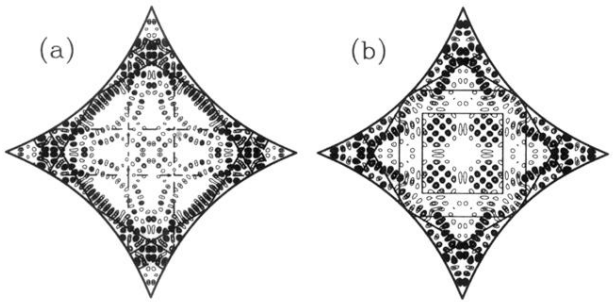

FIG. 5. The densities of the wave functions: (a) No. 94 scarred by the orbits $(+-)$ and $(+--)$; (b) No. 73 scarred by $(+-)$ and antiscarred by $(-)$.